

Experimental measurement of polyethylene chain modulus by scanning force microscopy

Binyang Du, Jieping Liu, Qingling Zhang, Tianbai He*

Polymer Physics Laboratory, Changchun Institute of Applied Chemistry, Chinese Academy of Sciences, Changchun, Jilin 130022, China

Dedicated to the memory of Professor Roger S. Porter.

Received 1 May 2000; received in revised form 1 December 2000; accepted 6 December 2000

Abstract

Nanoindentation technique and scanning force microscopy have been used to measure directly the polyethylene modulus along the chain axis. Single crystals of polyethylene were employed in order to obtain well-aligned chain segments. To minimize effects of scanner creep, a Z scan rate of 3 Hz was employed. The “X Rotate” value of 25° was selected to eliminate effects of lateral tip motion. The results were analyzed by the Oliver–Pharr method for which direct observation and measurement of the contact area are not required. Considering the influence of tip roundness on the projected contact area, the nanoindentation results were analyzed by the Sawa method. The chain modulus obtained from the thinner polyethylene single crystal sample was 204 ± 21 GPa by the Oliver–Pharr method and 168 ± 17 GPa by the Sawa method. The lower values than expected were due to substrate effects and anisotropy of chain deformation during nanoindentation. An extrapolation of the chain modulus obtained by various strains to zero nanoindentation eliminated the effect of substrate and anisotropy of chain deformation. The corresponding chain modulus obtained from the thicker sample was 278 GPa by the Oliver–Pharr method and 267 GPa by the Sawa method, respectively, in better agreement with the value of 340 GPa determined theoretically. © 2001 Elsevier Science Ltd. All rights reserved.

Keywords: Polyethylene single crystal; Nanoindentation; Scanning force microscopy

1. Introduction

With the use of polymers in ever more critical engineering applications, improved mechanical properties of them are necessary. Dr Porter has contributed dramatically to the improved mechanical properties of polymers [1] through his studies of chain orientation and alignment. Poly(4-methyl pentene-1) thin film with a modulus as high as half of its chain modulus was prepared in Dr Porter’s laboratory [2], for example. Estimating and measuring maximum mechanical behavior, i.e. chain modulus along the chain axis, are required to determine improvement of polymer mechanical properties. Although, reported by studies of maximum mechanical properties on polymers the measurements were not directly made by mechanical means [3,4]. Fabrication of large polymer samples with well-organized structure for studies by conventional mechanical instruments is difficult. With the advantage scanning force microscopy [5] even samples of small size may be employed. Since a

small polymer sample with well-aligned chain aggregation, for instance a polymer single crystal, can be easily fabricated, direct mechanical measurement for chain modulus using scanning force microscopy thus becomes possible.

Scanning force microscopy has since developed into a multifunctional technique suitable for characterization of surface morphology, mechanical and other properties, on the scale from hundreds of microns to nanometers, in a broad range of fundamental science and industrial applications it is employed [6,7]. For instance, nanomechanical properties such as hardness [8], elasticity [9] and viscoelasticity [10] of polymer thin films have been measured and compared with those in the bulk state. Little attention was devoted to the polymer modulus along its chain axis, referred to as the maximum polymer modulus. The mechanical improvement of polymeric materials became a focus of Dr Porter’s studies and he has made a significant contribution to this field. Single crystals of polyethylene were used as well-aligned chain aggregation samples. The nanoindentation technique and scanning force microscopy were employed for the direct measurement of the elastic modulus along the polyethylene chain axis.

* Corresponding author. Tel.: +86-431-568-2828 ext. 5402; fax: +86-432-568-5653.

E-mail address: tbhe@ns.ciac.ac.cn (T. He).

2. Experimental section

2.1. Sample preparation

Linear polyethylene with a weight-average molecular weight of 5800 Da and polydispersity of 1.1 was dissolved in xylene to obtain a 0.01 wt% solution. The solution was then kept in an oil bath with a crystallization temperature of 75°C controlled at $\pm 0.2^\circ\text{C}$ for 2 h followed by quenching to room temperature. A small amount of this solution with suspended single crystals was dropped onto a freshly cleaved mica surface and dried at room temperature for several days.

A metallocene-catalyzed short chain branched polyethylene (SCBPE) with butyl branches, weight-average molecular weight of 5910 Da and polydispersity of 1.1 was dissolved in xylene to obtain a 0.05 wt% solution. Thin film samples of SCBPE were obtained by solution casting onto freshly cleaved mica and placed on a hot stage fixed between two electrodes. Following application of high vacuum, the samples were heated to 160°C to ensure melt equilibrium. Electric field with an intensity of 18 kV/cm followed and the sample was kept constant for at least 3 h. The sample was then quickly cooled to the crystallization temperature of 125°C and kept for 10 h to form single crystals. The electric power was then shut and the samples were quickly cooled to room temperature.

2.2. Instrumentation

A Digital Instruments [11] NanoScope III^a Scanning Force Microscope with a diamond tip mounted on a stainless steel cantilever was utilized. The diamond tip is a Berkovich-like three-sided pyramid with an apex angle of about 60°, yielding a half-including angle of about 21.6° (the apex angle being the angle between a face and an edge of the pyramid.) The tip radius R is estimated by the supplier to be smaller than 25 nm, yielding a sufficiently sharp tip for nanoindentation [12]. The spring constant of the stainless steel cantilever is about 186 N/m.

Prior to nanoindentation, the polyethylene single crystal sample was imaged using a “tapping mode” to locate the area of interest. The “tapping mode” was then switched off and nanoindentation initiated. A load–deformation curve was recorded to deduce the sample’s mechanical property. Following nanoindentation, the indented sample was again imaged using the “tapping mode” and compared with the initial sample.

2.3. Nanoindentation technique

The indentation technique has been widely used for direct measurement of mechanical properties of the materials ranging from macroscale to nanometer scale [13]. The nanometer-scale indentation was employed as nano-indentation. The load–deformation curves obtained by nanoindentation were analyzed by the method proposed

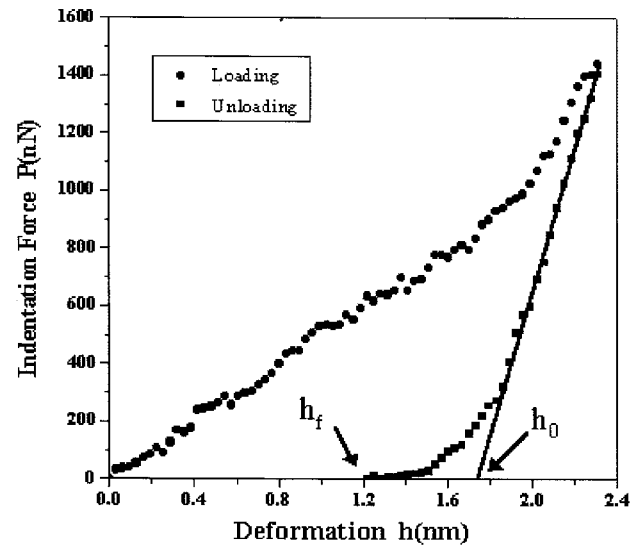


Fig. 1. A typical nanoindentation curve on a rhombic single crystal of linear polyethylene with a diamond tip. h_f : the permanent depth of the contact impression after unloading; h_0 : the plastic contact depth.

by Oliver and Pharr to consider elastic recovery of the sample during nanoindentation [14]. The speciality of this approach is that the direct observation and measurement of the contact area are not necessary for evaluation of elastic modulus. In order to calculate the indentation force and indentation depth of the sample as accurately as possible, the detection sensitivity (or cantilever sensitivity) was measured on a “infinitely stiff” sapphire sample before and after nanoindentation. Fig. 1 presents a typical nanoindentation curve on a polyethylene single crystal. The effective elastic modulus E_{eff} of the sample can be calculated by:

$$E_{\text{eff}} = \frac{1}{\beta} \frac{\sqrt{\pi}}{2} \frac{S}{\sqrt{A}} \quad (1)$$

where A is the projected contact area, S the unloading stiffness and value of β taken as 1.034 for a Berkovich indentation tip. If the elastic deformation occurring in both the specimen and indentation tip are taken into account, the effective modulus is given by

$$\frac{1}{E_{\text{eff}}} = \frac{(1 - \nu_t^2)}{E_t} + \frac{(1 - \nu_s^2)}{E_s} \quad (2)$$

where E_s and ν_s are Young’s modulus and Poisson’s ratio for the sample, and E_t and ν_t the same quantities for the indentation tip, respectively. $E_t = 1141$ GPa and $\nu_t = 0.07$ for a diamond tip. The projected contact area A in Eq. (1) is derived from the indentation tip shape function at the contact depth h_c with $A = f(h_c)$. For a perfect Berkovich indentation tip, the projected contact area is given by

$$A = 24.5 h_c^2 \quad (3)$$

and the contact depth h_c given by

$$h_c = h_{\max} - \varepsilon \frac{P_{\max}}{S} \quad (4)$$

where h_{\max} is the maximum indentation deformation at maximum indentation force P_{\max} , and the value of ε is taken as 0.75 for the Berkovich indentation tip. The unloading stiffness, $S = dP/dh$ ($h = h_{\max}$), and the slope of the initial linear portion of the unloading curve is approximated by the function

$$P = B(h - h_f)^m \quad (5)$$

where P is the indentation force, h the deformation, B and m are fitting parameters and h_f the permanent deformation remained after complete unloading. With known values of B and m the derivative dP/dh ($h = h_{\max}$) of the function (5) can be obtained.

3. Results and discussion

3.1. Influence of experimental parameters

Since the piezoelectric scanner used has shown creep behavior and introduced uncertainties in measurement [15], the effects of such creep were observed and are presented in Fig. 2. As the detection sensitivity remained approximately constant with a Z scan rate higher than 3 Hz, a Z scan rate of 3 Hz was selected for nanoindentation measurements to minimize the effect of scanner creep.

A possible additional lateral tip motion during nanoindentation due to scanning force microscopy design whereby the tip was mounted on a stainless steel cantilever with a certain angle of 12° to the horizontal has been reported [12]. To compensate for the effect of lateral tip motion on nanoindentation measurements, new software has been developed by Digital Instruments to set an “X Rotate” parameter [12]. The “X Rotate” parameter prevents the tip from plowing on the surface laterally, typically along the x -direction, while it

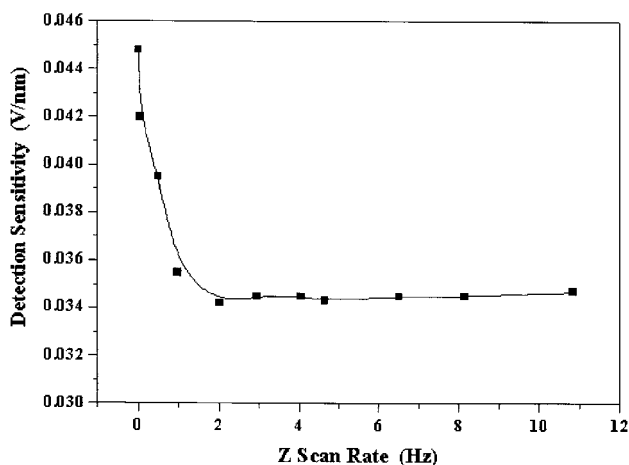


Fig. 2. Detection sensitivity of nanoindentation on sapphire sample with a diamond tip as a function of the Z scan rate.

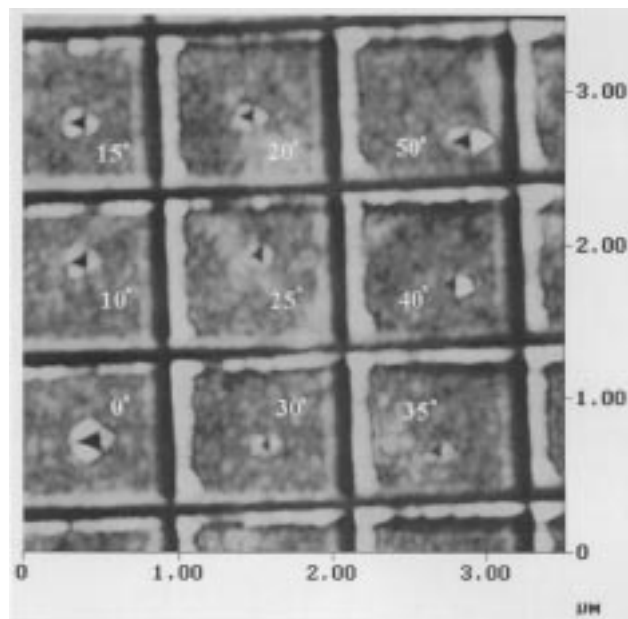


Fig. 3. TM AFM image of gold sample after nanoindentation with increasing lateral compensation.

indents on the sample surface in the z -direction. The “X Rotate” parameters with 0° , 10° , 15° , 20° , 25° , 30° , 35° , 40° and 50° were tested on a gold surface. Increasing the “X Rotate” parameter was found to decrease the deformation area (Fig. 3). The values of “X Rotate” parameters between 25° and 30° created the smallest indented local area, indicative of tip motion vertically with respect to the local sample. A further increase of “X Rotate” parameters results in over-compensation due to the apparent pile-up on the right side of the local indented area. A value of 25° was selected for nanoindentation measurements to eliminate effects of lateral tip motion.

3.2. Chain modulus of polyethylene single crystals

Fig. 4 presents a transmission electron microscope of a single crystal of linear polyethylene of rhombic shape formed from dilute xylene solution. The orthorhombic chain packing structure with $a = 0.751$ nm and $b = 0.505$ nm was identified from electron diffraction. The rhombic single crystal of about 10–11 nm thickness was measured by scanning force microscopy.

Fig. 5a and b present the morphology of a typical rhombic single crystal before and after nanoindentation on the surface of the single crystal vertical to plane (001) with the same indentation force of about $1.4 \mu\text{N}$. The data obtained from nanoindentation 16 times on a different location of the same sample is shown in Table 1. The Oliver–Pharr method (Eqs. (1)–(5)) was used to analyze nanoindentation data and calculate modulus. Note the pile-up of polyethylene sample around the indentation tip which may influence the accuracy of contact area and elastic

modulus measurements. It has been reported that the ratio of permanent indentation depth, h_f to the depth of the nanoindentation at peak load, h_{max} , i.e. h_f/h_{max} , was a criterion. Usually $0 \leq h_f/h_{max} \leq 1$. The lower ratio corresponds to fully elastic deformation; the larger ratio to rigid-plastic behavior. When $h_f/h_{max} < 0.7$, i.e. the pile-up of material around the indenter was smaller, the contact areas obtained by the Oliver–Pharr method agree well with that obtained from finite element analyses. The Oliver–Pharr method led to large errors when $h_f/h_{max} > 0.7$ [16,17]. In this work h_f/h_{max} ratios were about 0.4–0.6 for all measurements. The modulus measured from the rhombic single crystal sample by Eqs. (1)–(3) is 204 ± 21 GPa (Table 1). The Poisson's ratio was taken as 0.41 [18].

The roundness of the indentation tip has been reported to influence the nanoindentation measurement. Use of a perfect Berkovich indentation tip results in underestimation of the real projected contact area and overestimation of elastic modulus [19]. Since the tip used in this work is sharper, the influence of tip roundness on the real projected contact area should be considered. According to Sawa et al. [20] the real projected contact area A_r for nanoindentation of a thin film using a three-sided pyramid indentation tip is given by

$$A_r = 3\sqrt{3}(\tan^2 \alpha)(h_0 + \Delta h_T)^2 \quad (6)$$

$$\Delta h_T = (R/8) \cot^2 \alpha \quad (7)$$

where R and α are the tip radius and half-including angle of a three-sided pyramid indentation tip, and h_0 the plastic contact depth shown in Fig. 1. Based on a nanoindentation measurement on Si(111) with elastic modulus of 130 GPa

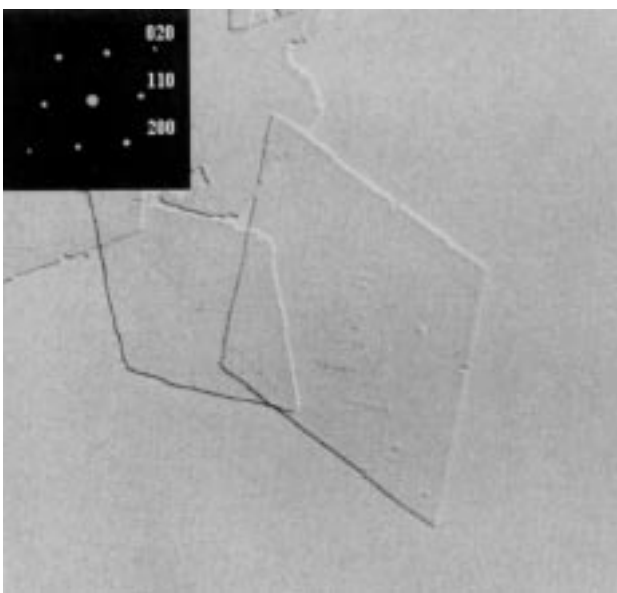


Fig. 4. TEM micrograph of the rhombic single crystal of linear polyethylene formed from dilute xylene solution. The inset is electron diffraction.

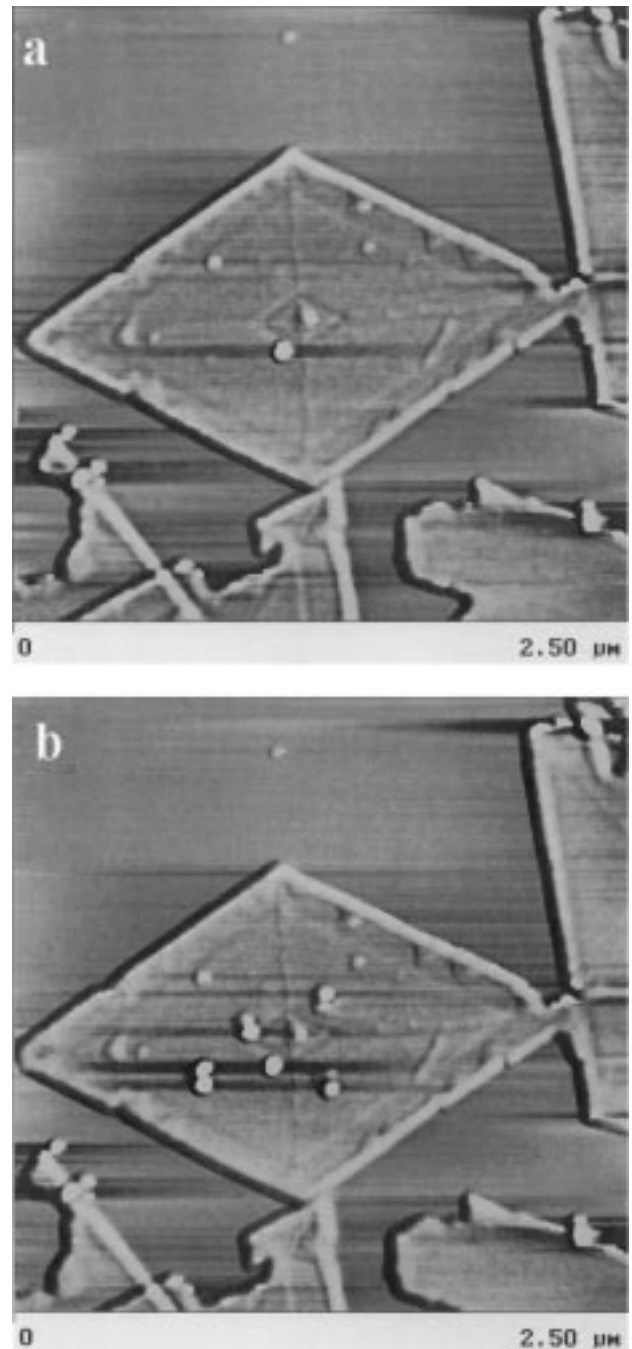


Fig. 5. TM AFM image of a rhombic single crystal of linear polyethylene. (a) before and (b) after nanoindentation with indentation force of about $1.4 \mu\text{N}$.

using the method of Sawa et al. [20], the Δh_T of about 10.37 nm was obtained for the tip used here. Accordingly, the three-sided pyramid indentation tip used is of tip radius R of about 13 nm and half-including angle of about 21.6° . From the real projected contact area A_r obtained from the values of tip radius and half-including angle, a calibrated elastic modulus E_r of the sample by Eqs. (6) and (7) was 168 ± 17 GPa (Table 1).

Polyethylene chain modulus along its chain axis E_{max}

Table 1

Chain modulus measured in rhombic polyethylene single crystal by nanoindentation with indentation force of about 1.4 μN

No.	$h_0(\text{nm})$	$h_f(\text{nm})$	h_{max}	h_f/h_{max}	E (GPa)	E_r (GPa)
1	1.75	1.22	2.31	0.53	238	197
2	1.74	1.13	2.37	0.48	192	158
3	1.76	1.24	2.44	0.51	171	142
4	1.69	1.26	2.31	0.55	207	170
5	1.89	1.36	2.36	0.57	240	195
6	1.71	1.30	2.37	0.55	186	154
7	1.91	1.27	2.41	0.53	219	180
8	1.78	1.23	2.41	0.51	176	144
9	1.74	1.15	2.37	0.49	184	154
10	1.96	1.31	2.48	0.53	207	173
11	1.74	1.14	2.38	0.48	191	157
12	1.79	1.24	2.36	0.53	230	189
13	1.72	1.22	2.33	0.52	194	155
14	1.90	1.33	2.43	0.55	216	180
15	1.77	1.30	2.37	0.55	203	165
16	1.69	1.25	2.33	0.54	206	167
Average	–	–	–	–	204 ± 21	168 ± 17

ranging from 240 to 358 GPa has been determined by various methods [21–24]. The lowest value of 240 GPa obtained by X-ray diffraction [24] is still larger than that obtained by nanoindentation in this work and results from anisotropy of chain deformation during nanoindentation. Plastic deformation or yielding may occur during nanoindentation, resulting in plastic flow along any direction with regards to the chain axis. For instance, a typical direction was perpendicular to the chain axis. Since the chain modulus vertical to the chain axis is about 4.3 GPa for polyethylene [24], far lower than that along the chain axis, the contribution of the plastic flow in such directions reduces the mechanical response. Thus, the measured value of the elasticity along the chain axis is decreased by the plastic flow in such directions, which may explain our lesser value of chain modulus.

3.3. Substrate effect

It has been reported that when the indentation depth exceeds 10–25% of sample thickness, the effect of substrate on the measurement should be considered [25]. Since the thickness of the rhombic single crystal sample used for modulus measurements in Table 1 is about 10–11 nm, the appropriate indentation depth should be less than 1 nm and the corresponding indentation force is about 1.4 μN . This less force value on the edge of the instrument used. The typical indentation force of the instrument ranges from 1–100 μN with a resolution of 0.5 μN [12]. To eliminate the effect of substrate, two methods can be employed: one is to increase the resolution of the instrument, which is impossible in this case, and the other is to increase the sample thickness.

Fig. 6 presents a transmission electron microscope of a single crystal of branched polyethylene with circular shape

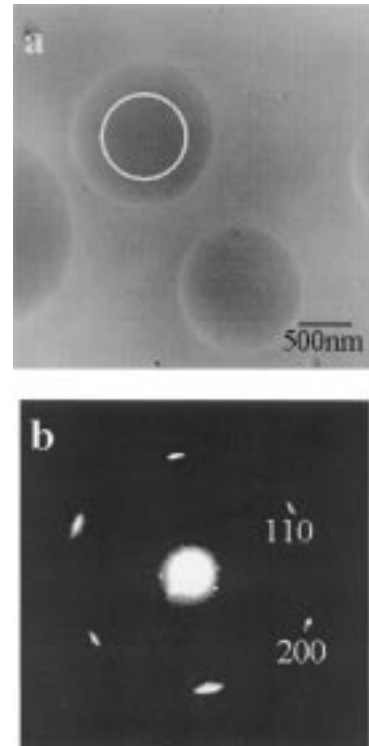


Fig. 6. TEM micrograph of (a) the morphology of the circular single crystal of branched polyethylene formed from melt under electric field and (b) electron diffractions.

and formed from the melt under an electric field [26]. The orthorhombic chain packing structure with $a = 0.828$ nm and $b = 0.496$ nm was identified from electron diffraction. The circular single crystal of about 50 nm center thickness was measured by scanning force microscopy.

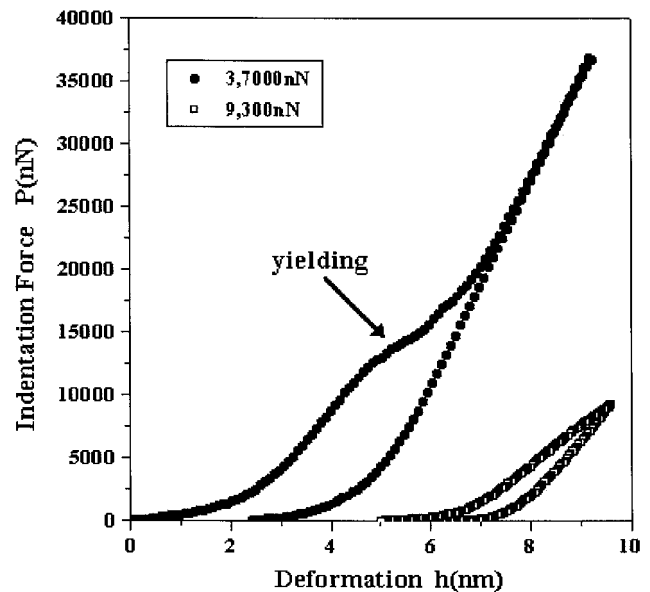


Fig. 7. Two typical nanoindentation curves on a circular single crystal of branched polyethylene with indentation force of 37 and 9.3 μN , respectively.

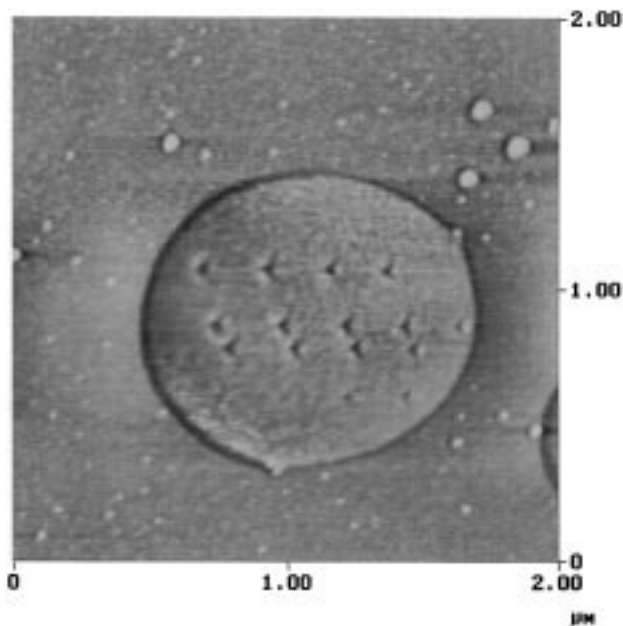


Fig. 8. TM AFM image of a series of nanoindentation on circular single crystal of branched polyethylene with various indentation force.

Two typical nanoindentation curves on the top surface of a circular single crystal of different indentation force are shown in Fig. 7. A yield in the loading portion of the nanoindentation curve with as large an indentation force as $37 \mu\text{N}$ is clearly seen. This observation indicates that the chain deformation from such a load–deformation curve is not linear and the chain modulus determined thereafter is questionable. When the indentation force was reduced to as low as $9.3 \mu\text{N}$, yielding did not occur. Thus, nanoindentation with various indentation depths, i.e. indentation strains, is preferable followed by assignment of the modulus extrapolated to the zero indentation strain as sample modulus. Fig. 8 shows the TM AFM image of a series of nanoindentations on circular single crystals of branched polyethylene with various indentation force. The relationship between elastic modulus and indentation strain ε , ratio of the permanent indentation depth to sample thickness, is shown in Fig. 9. This figure indicates the extrapolated value of the chain modulus determined by Eqs. (1)–(3) is 278 GPa, and that by Eqs. (1), (2) and (6) is 267 GPa.

The extrapolated values of chain modulus shown in Fig. 9 better match those of 340 GPa determined theoretically [21]. The extrapolation considers both the effect of substrate and linear deformation. Further work is required to obtain a direct mechanical measurement for chain modulus of polymers with more accuracy. Such studies are being pursued in the field of micro- and nano-mechanics of the materials [27].

4. Conclusions

The nanoindentation technique was used to obtain a direct

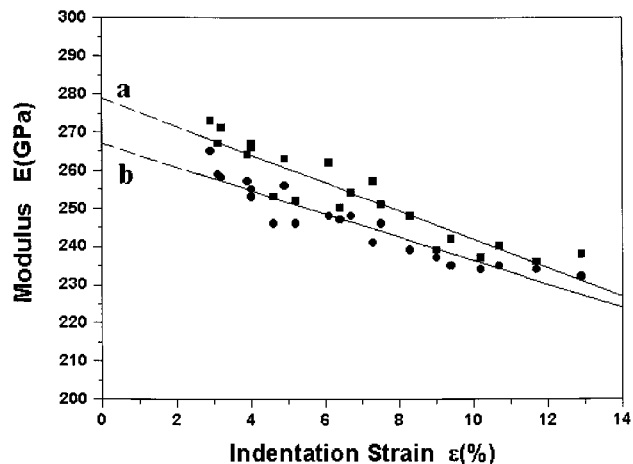


Fig. 9. The relationship between the elastic modulus E and the indentation strain ε of circular single crystal of branched polyethylene. The extrapolated values to the zero indentation strain as the chain modulus of the sample measured.

mechanical measurement for chain modulus of polyethylene along its chain axis. The chain modulus obtained from the polyethylene sample of thinner thickness were 204 ± 21 GPa by Oliver–Pharr method and 168 ± 17 GPa by Sawa method, respectively. The lower values than expected values are due to the effects of the substrate and anisotropy of chain deformation during nanoindentation. An extrapolation of the chain modulus obtained by various nanoindentation strains to zero nanoindentation was used to eliminate the effect of substrate and anisotropy of chain deformation. The corresponding chain modulus obtained from polyethylene samples of thickness were 278 GPa by Oliver–Pharr method and 267 GPa by Sawa method, respectively, in better agreement with the value of 340 GPa determined theoretically. Further efforts are needed to improve direct mechanical measurements for polymer chain modulus with more accuracy and to design new polymers with well-known chain mechanical properties for a variety of technological applications.

Acknowledgements

This work was supported by the National Science Foundation of China and subsidized by Special Funds for Major State Basic Research Projects of China. Polyethylene samples from Phillips Petroleum Company were kindly supplied by Stephen Z.D. Cheng at the University of Akron. Drs S. Magonov and L. Huang of Digital Instruments kindly supplied the sapphire sample for calibrating the detection sensitivity of SFM.

References

- [1] Porter RS, Wang LH. JMS — Rev Macromol Chem Phys C 1995;35:63–115.

- [2] He T, Porter RS. *Polymer* 1987;28:946–50 (see also p. 1321–5).
- [3] He T. *Polymer* 1986;27:253–5.
- [4] He T. *Makromol Chem* 1987;188:2489–94.
- [5] Binnig G, Quate CF, Gerber C. *Phys Rev Lett* 1986;56:930–3.
- [6] Magonov SN, Reneker DH. *Annu Rev Mater Sci* 1997;27:175–222.
- [7] Radmacher M, Tillmann RW, Fritz M, Gaub HE. *Science* 1992;257:1900–5.
- [8] Drechsler D, Karbach A, Fuchs H. *Appl Phys A* 1998;66:S825–9.
- [9] Domke J, Radmacher M. *Langmuir* 1998;14:3320–5.
- [10] Tanaka K, Takahara A, Kajiyama T. *Macromolecules* 1998;31:863–9.
- [11] Digital Instruments Inc., NanoScope III^a, MultiMode™ scanning probe microscope instruction manual, Santa Barbara, CA, 1997.
- [12] Digital Instruments Inc., Support note no. 225, Rev F, Santa Barbara, CA, 1998.
- [13] Pharr GM. *Mater Sci Engng A* 1998;253:151–9.
- [14] Oliver WC, Pharr GM. *J Mater Res* 1992;7:1564–83.
- [15] Hues SM, Draper CF, Colton RJ. *J Vac Sci Technol B* 1994;12:2211–4.
- [16] Bolshakov A, Oliver WC, Pharr GM. *J Mater Res* 1996;11:760–8.
- [17] Bolshakov A, Pharr GM. *J Mater Res* 1998;13:1049–58.
- [18] Choy CL, Leung WP. *J Appl Polym Sci* 1986;32:5883–901.
- [19] Murakami Y, Tanaka T, Itokazu M, Shimamoto A. *Philos Mag* 1994;69:1131–53.
- [20] Sawa T, Akiyama Y, Shimamoto A, Kohichi T. *J Mater Res* 1999;14:2228–32.
- [21] Shimanouchi TJ, Asahina M, Enimoto S. *J Polym Sci* 1962;59:93–100.
- [22] Shauffele RF, Shimanouchi T. *J Chem Phys* 1967;47:3605–10.
- [23] Capaccio G, Ward IM. *Polym Engng Sci* 1975;15:219–24.
- [24] Sakurada I, Ito T, Nakamae K. *J Polym Sci C* 1966;15:75–91.
- [25] Pharr GM, Oliver WC. *MRS Bull* 1992;17:28–33.
- [26] Liu J, Xie F, Du B, Zhang F, Zhang Q, He T. In: *Preprints of 6th Pacific Polym Conf*, 1999. p. 186.
- [27] *Workshop on Nano and Micromechanics of Solids for Emerging Science and Technology by NSF*, Palo Alto, California, USA, 1999.